

Multi-orbital Flat Band Ferromagnetism with a Provable Percolation Representation

Eric Bobrow, Junjia Zhang, and Yi Li*

Department of Physics and Astronomy, Johns Hopkins University, Baltimore, Maryland 21218, USA

(Dated: November 20, 2020)

We consider a two-layer multi-orbital system consisting of a p_x, p_y -orbital honeycomb lattice layer and an f -orbital triangular lattice layer with sites aligned with the centers of the honeycomb plaquettes. With an appropriately tuned chemical potential difference between these two layers, the system exhibits a flat band with provably ferromagnetic ground states at half filling of the band in the presence of intra-orbital Hubbard interactions and Hund's coupling. Away from half filling, the interacting system admits a percolation representation, where the ground state space is spanned by maximum-spin clusters of localized single-particle states. A paramagnetic-ferromagnetic transition occurs as the band approaches half filling and the ground states become dominated by states with a large cluster.

I. INTRODUCTION

Systems with flat bands can exhibit many interesting physical properties, including ferromagnetism and exotic correlated states, where the flat band enhances interaction effects, as well as topology in non-interacting flat bands [1–12]. In many models of flat band systems, the flat band can be attributed to a large number of degenerate states that are localized due to destructive interference. Tight-binding models on line graphs [2] as well as decorated lattices such as the Tasaki lattice [13] feature flat bands that can be understood in terms of a cell construction [14] with destructively interfering hopping. In the presence of a repulsive on-site Hubbard interaction, these models exhibit saturated ferromagnetism when the flat band is half filled [1, 15]. For certain models such as the Tasaki lattice, the intuition that overlapping single-particle states maximize spin to avoid the repulsive interaction holds even below half filling, where the interacting ground states are spanned by product states formed from clusters of localized single-particle states, with the clusters independently maximizing spin [1, 16]. Since the total spin of each cluster depends only on its size, the result is a percolation representation that can be efficiently simulated to find the transition from paramagnetic states with small clusters at low filling to ferromagnetic states with large clusters at high filling [17, 18].

Flat bands can also be realized in orbital-active systems, where orbital-dependent hopping can prevent states from dispersing. A particular example of this is the honeycomb lattice with p_x and p_y orbitals at each site and orbital-dependent hopping along the bond directions, where it was shown in Ref. [3] that both the lowest and highest bands are flat. The flat bands are spanned by loop states around each honeycomb where each site on the loop features a superposition of p_x and p_y orbitals to form a p orbital perpendicular to the outgoing bond that cannot hop out due to the bond-projected hopping.

In order to find a percolation representation, Ref. [1]

considers a flat band with a basis of single-particle states that are *quasilocal*, meaning each basis state is nonzero on a site where all other basis states vanish. When a positive Hubbard U interaction is turned on, the quasilocality condition prevents double occupation of single-particle states. When the basis satisfies the additional requirement that no more than two quasilocal states overlap at any site, Hubbard interaction causes the overlapping states to maximize spin. Breaking these conditions can introduce additional states into the interacting ground state space that have lower spin within the cluster, making the percolation picture non-rigorous. For the p_x - and p_y -orbital model of Ref. [3] together with an intra-orbital Hubbard interaction, the loop states violate both conditions, with two or three loop states overlapping in every orbital.

In this article, we study a two-layer system consisting of a p_x - and p_y -orbital honeycomb layer together with a triangular lattice f -orbital layer. When the chemical potential of the f -orbital layer is appropriately tuned, the system features a flat band spanned by localized states centered on each f orbital. We show that when this band is the highest energy band, the system admits a percolation representation in the presence of Hund's coupling between the p orbitals despite violating the condition in Ref. [1] that at most two states overlap on site.

The remainder of this article is organized as follows. In Section II, we introduce the multi-orbital model, find the condition under which the model admits two bands, and discuss the localized single-particle states. In Section III, we first review the percolation representation in Ref. [1] and then extend it to our multi-orbital system with Hund's coupling.

II. MODEL HAMILTONIAN

The model Hamiltonian consists of spin-1/2 electrons in a two-layer system with one layer a p_x, p_y -orbital honeycomb lattice and the other a triangular f -orbital lattice with one $f_{y(3x^2-y^2)}$ orbital per site. The f -orbital lattice is arranged such that the f orbitals are aligned with the centers of the p -orbital honeycomb cells. The set of p -

* yili.phys@jhu.edu

orbital and f -orbital sites will respectively be labeled Λ_p and Λ_f , with these disjoint sets partitioning the overall lattice $\Lambda = \Lambda_p \sqcup \Lambda_f$.

The kinetic Hamiltonian is $H_K = H_K^p + H_K^f + H_K^{fp}$ with p -orbital part

$$H_K^p = t_p \sum_{\mathbf{r} \in \Lambda_p^A} \sum_{\sigma=\uparrow,\downarrow} \sum_{i=1}^3 p_{\mathbf{r}+\mathbf{v}_i, \sigma}^\dagger p_{\mathbf{r}, \sigma} + h.c., \quad (1)$$

where Λ_p^A is the A sublattice of the p -orbital layer and $p_{\mathbf{r}, \mathbf{v}_i, \sigma} = \hat{v}_i \cdot \mathbf{p}_{\mathbf{r}, \sigma}$ is the projection of the p_x, p_y orbitals at site \mathbf{r} in the bond direction $\hat{\mathbf{v}}_i$, describing sigma bonding. The vectors \mathbf{v}_i are the nearest neighbor vectors $\mathbf{v}_1 = (1, 0)$, $\mathbf{v}_2 = (-\frac{1}{2}, \frac{\sqrt{3}}{2})$, $\mathbf{v}_3 = (-\frac{1}{2}, -\frac{\sqrt{3}}{2})$. Here we take the honeycomb lattice bond length to be 1. This p_x - p_y orbital model has been previously discussed in Refs. [3, 19, and 20]. The f orbital layer forms a triangular lattice with sites \mathbf{R} aligned with the centers of the p -orbital honeycombs and are described by the kinetic Hamiltonian

$$H_K^f = t_f \sum_{\mathbf{R} \in \Lambda_f} \sum_{\sigma=\uparrow,\downarrow} \sum_{i=1}^6 f_{\mathbf{R}+\mathbf{w}_i, \sigma}^\dagger f_{\mathbf{R}, \sigma} + h.c., \quad (2)$$

where \mathbf{w}_i are the six nearest-neighbor vectors on the f -orbital triangular lattice, $w_i = \sqrt{3}(\cos \phi_i, \sin \phi_i)$ with $\phi_i = \frac{\pi}{6}(2i-1)$ and $i = 1, \dots, 6$.

Hopping between layers is described by

$$H_K^{fp} = t_{fp} \sum_{\mathbf{R} \in \Lambda_f} \sum_{\sigma=\uparrow,\downarrow} \sum_{i=1}^6 (-1)^{i-1} f_{\mathbf{R}, \sigma}^\dagger p_{\mathbf{R}+\mathbf{u}_i, \mathbf{u}_i^\perp, \sigma} + h.c. \quad (3)$$

where $\mathbf{u}_i = (\cos \theta_i, \sin \theta_i)$ with $\theta_i = \frac{\pi}{3}(i-1)$, a reordering of the \mathbf{v} vectors. In particular, $\mathbf{R} + \mathbf{u}_i \in \Lambda_p$ when $\mathbf{R} \in \Lambda_f$. Here \mathbf{u}_i^\perp are defined to be unit vectors perpendicular to \mathbf{u}_i^\perp with sign chosen so that \mathbf{u}_{i+1}^\perp is a $\pi/3$ rotation of \mathbf{u}_i^\perp . Thus, $\mathbf{u}_i^\perp = (-\sin \theta_i, \cos \theta_i)$. The alternating sign in the hopping amplitude is due to the fact that the $f_{y(3x^2-y^2)}$ orbital changes sign under $\frac{\pi}{3}$ rotation. To interpret the model as a two-layer system, the \mathbf{u}_i vectors can be thought of as the xy -plane component of the vector between the f orbitals on Λ_f and the adjacent p orbitals on Λ_p , with the z component being a small inter-layer distance.

Typical hopping terms are depicted in Fig. 1(a), which shows that hopping between p orbitals with amplitude t_p occurs between superpositions of p_x and p_y aligned along the bond direction and hopping between p and f orbitals involves superpositions of p orbitals aligned perpendicular to the in-plane hopping direction. Since the p and f orbitals are odd under inversion, we take all hopping parameters to be positive, $t_p, t_f, t_{fp} > 0$.

In addition to the off-diagonal kinetic terms, we consider chemical potential shifts for the p and f orbital layers,

$$H_\mu = -\mu_p \hat{N}_p - \mu_f \hat{N}_f, \quad (4)$$

where the total number operator for p -orbital electrons is $\hat{N}_p = \sum_{\mathbf{r} \in \Lambda_p} \sum_{p=p_x, p_y} \sum_{\sigma=\uparrow,\downarrow} n_{\mathbf{r}, p, \sigma}$ with $n_{\mathbf{r}, p_x, \sigma} = p_{\mathbf{r}, \hat{x}, \sigma}^\dagger p_{\mathbf{r}, \hat{x}, \sigma}$ and a similar expression for $n_{\mathbf{r}, p_y, \sigma}$. The total number operator for f -orbital electrons is defined similarly, $\hat{N}_f = \sum_{\mathbf{R} \in \Lambda_f} \sum_{\sigma=\uparrow,\downarrow} n_{\mathbf{R}, f, \sigma}$ with $n_{\mathbf{R}, f, \sigma} = f_{\mathbf{R}, \sigma}^\dagger f_{\mathbf{R}, \sigma}$.

The on-site intra-orbital Coulomb interaction is described by the Hubbard U terms for p and f orbitals. Written in a particle-hole-symmetric form, the interaction Hamiltonian H_U is

$$H_U = U_p \sum_{\mathbf{r} \in \Lambda_p} \sum_{p=p_x, p_y} \left(n_{\mathbf{r}, p, \uparrow} - \frac{1}{2} \right) \left(n_{\mathbf{r}, p, \downarrow} - \frac{1}{2} \right) + U_f \sum_{\mathbf{R} \in \Lambda_f} \left(n_{\mathbf{R}, f, \uparrow} - \frac{1}{2} \right) \left(n_{\mathbf{R}, f, \downarrow} - \frac{1}{2} \right), \quad (5)$$

which can also be written in terms of $H'_U = U_p \sum_{\mathbf{r} \in \Lambda_p} \sum_{p=p_x, p_y} n_{\mathbf{r}, p, \uparrow} n_{\mathbf{r}, p, \downarrow} + U_f \sum_{\mathbf{R} \in \Lambda_f} n_{\mathbf{R}, f, \uparrow} n_{\mathbf{R}, f, \downarrow}$ as $H_U = H'_U - \frac{U_p}{2} \hat{N}_p - \frac{U_f}{2} \hat{N}_f + \frac{2U_p|\Lambda_p| + U_f|\Lambda_f|}{4}$. We will consider only the repulsive case with $U_p, U_f > 0$.

As we will see, the intra-orbital Hubbard interactions alone are not sufficient for the percolation representation we discuss in Section. III B. The ability of the Hund's coupling in multi-orbital systems to polarize electrons in degenerate orbitals will be essential. The on-site Hund's coupling between p_x and p_y orbitals is

$$H_J = -J \sum_{\mathbf{r} \in \Lambda_p} \left(\mathbf{S}_{\mathbf{r}, p_x} \cdot \mathbf{S}_{\mathbf{r}, p_y} - \frac{1}{4} n_{\mathbf{r}, p_x} n_{\mathbf{r}, p_y} \right), \quad (6)$$

where $S_{\mathbf{r}, p_x/y}^i = \frac{1}{2} \sum_{\mu, \nu=\uparrow, \downarrow} p_{\mathbf{r}, \hat{x}/\hat{y}, \mu}^\dagger \sigma_{\mu\nu}^i p_{\mathbf{r}, \hat{x}/\hat{y}, \nu}$ with Pauli matrices σ^i , $i = x, y, z$, and the Hund's coupling $J > 0$. The number operators without a spin index count both spin up and down, such as $n_{\mathbf{r}, p_x} = \sum_{\sigma=\uparrow, \downarrow} n_{\mathbf{r}, p_x, \sigma}$. The Hund's coupling energy from two electrons in an inter-orbital singlet state at a site \mathbf{r} is thus J , with an on-site triplet state having 0 Hund's coupling energy.

In the absence of the hoppings between f - and p -orbitals, the decoupled p -orbital Hamiltonian in Eq. (1), together with the chemical potential, features two flat bands with energies $E_{p, \pm} = \pm \frac{3}{2} t_p - \mu_p$ as discussed in Refs. [3, 19, and 20]. The lower flat band is spanned by localized p -orbital loops with alternating sign $|\psi_{\mathbf{R}, \sigma}^{-(p)}\rangle = \frac{1}{\sqrt{6}} \sum_{i=1}^6 (-1)^{i-1} p_{\mathbf{R}+\mathbf{u}_i, \mathbf{u}_i^\perp, \sigma}^\dagger |0\rangle$ on each honeycomb, where the f orbital site $\mathbf{R} \in \Lambda_f$ is used to label the surrounding honeycomb. The upper flat band is spanned by $|\psi_{\mathbf{R}, \sigma}^{+(p)}\rangle = \frac{1}{\sqrt{6}} \sum_{i=1}^6 p_{\mathbf{R}+\mathbf{u}_i, \mathbf{u}_i^\perp, \sigma}^\dagger |0\rangle$. These loop states feature a superposition of p_x and p_y orbitals to form a p orbital perpendicular to the outgoing bond that cannot hop out due to the bond-projected hopping. These states can also be thought of as localized due to destructive interference in the p_x - p_y basis.

In the presence of the f - and fp -orbital hopping terms, these flat band states can be extended to the full system.

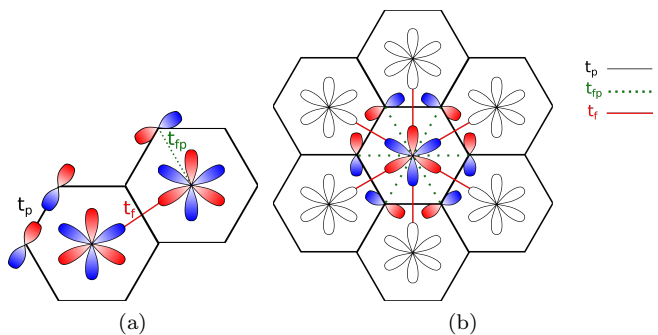


FIG. 1. Top view of the two-layer lattice. Red and blue respectively denote positive and negative lobes for the p - and f -orbital wavefunctions. (a) Examples are shown of hopping t_f between f orbitals, t_p between p orbitals along the honeycomb bond direction, and t_{fp} between f and p orbitals perpendicular to the hopping direction. (b) A localized state formed by a superposition of an f orbital and a surrounding loop of p orbitals with alternating signs.

In general, H_{fp} mixes the p - and f -orbital bands, potentially distorting the p -orbital flat bands. We can find conditions under which the bands remain flat by first assuming $|\psi_{\mathbf{R},\sigma}\rangle \equiv a|\psi_{\mathbf{R},\sigma}^{-(p)}\rangle + b|f_{\mathbf{R},\sigma}\rangle$ and choosing coefficients a, b such that $|\psi_{\mathbf{R},\sigma}\rangle$ is an eigenstate of H_K ,

$$\begin{aligned} H_K|\psi_{\mathbf{R},\sigma}\rangle &= (E_{p,-} - \mu_p)a|\psi_{\mathbf{R},\sigma}^{-(p)}\rangle + 6t_{fp}a|f_{\mathbf{R},\sigma}\rangle \\ &\quad + t_{fp}b|\psi_{\mathbf{R},\sigma}^{-(p)}\rangle - \mu_f b|f_{\mathbf{R},\sigma}\rangle \\ &\quad + (-at_{fp} + bt_f) \sum_{i=1}^6 |f_{\mathbf{R}+\mathbf{w}_i,\sigma}\rangle \\ &= E_{fp}|\psi_{\mathbf{R},\sigma}\rangle. \end{aligned} \quad (7)$$

The state $|\psi_{\mathbf{R},\sigma}\rangle = t_f/\mathcal{N}_t|\psi_{\mathbf{R},\sigma}^{-(p)}\rangle + t_{fp}/\mathcal{N}_t|f_{\mathbf{R},\sigma}\rangle$ with normalization $\mathcal{N}_t = \sqrt{t_f^2 + t_{fp}^2}$ is an eigenstate with energy $E_{fp} = -(3/2)t_p - \mu_p + t_{fp}^2/t_f$ when the chemical potential difference $\mu_f - \mu_p$ takes a critical value. As this can also be thought of as tuning μ_f with μ_p fixed, we will consider the f orbital critical chemical potential

$$\mu_f^c \equiv \mu_p + 6t_f + \frac{3}{2}t_p - \frac{t_{fp}^2}{t_f}, \quad (8)$$

which can be satisfied in principle for any hopping amplitude values t_p, t_f, t_{fp} . The localized states $|\psi_{\mathbf{R},\sigma}\rangle$ at different \mathbf{R} then span a flat band with energy E_{fp} .

One interesting feature of the model is that, for symmetry reasons, the upper flat band of H_K^p remains flat in the presence of H_K^f and H_K^{fp} with energy $E_{p,+} = \frac{3}{2}t_p - \mu_p$, since the states $|\psi_{\mathbf{R},\sigma}^{+(p)}\rangle$ centered at each honeycomb \mathbf{R} destructively interfere at $|f_{\mathbf{R}}\rangle$ as well as at the neighboring f orbitals. This flat band requires no chemical potential tuning, though whether it is the highest band of H_K depends on the hopping amplitudes.

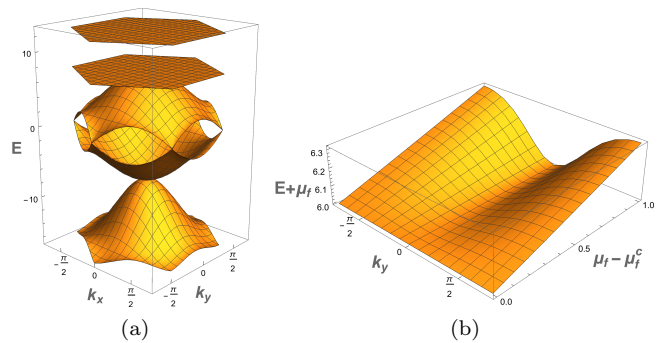


FIG. 2. For $\mu_p = 0$, $t_p = 5$, $t_f = 1$, and $t_{fp} = 4.5$, plots are shown of (a) the band structure of H_K in the first Brillouin zone with $\mu_f = \mu_f^c$ and (b) the energy of the top band as a function of k_y and μ_f . At $\mu_f = \mu_f^c$, the top band is flat.

When $\mu_f = \mu_f^c$, there are five bands including the two flat bands at energies E_{fp} and $E_{p,+}$ and three dispersive bands with energies

$$\begin{aligned} E_{2,\pm}(\mathbf{k}) &= -\mu_p \pm \frac{t_p}{2} \sqrt{4 \cos \frac{3k_x}{2} \cos \frac{\sqrt{3}k_y}{2} + 2 \cos \sqrt{3}k_y + 3} \\ E_1(\mathbf{k}) &= -\frac{3t_p}{2} - \mu_p \\ &\quad + 2t_f \left(2 \cos \frac{3k_x}{2} \cos \frac{\sqrt{3}k_y}{2} + \cos \sqrt{3}k_y - 3 \right). \end{aligned} \quad (9)$$

In fact, $E_{2,\pm}$ are exactly the dispersive bands of the p -orbital model H_K^p [3]. When $\mu = \mu_f^c$, the addition of the f -orbital layer leaves the dispersive bands and one flat band, $E_{p,+}$, of the p -orbital layer unchanged, while introducing a dispersive band $E_1(\mathbf{k})$ and involving f orbitals in the remaining flat band E_{fp} . These five bands are shown in the first Brillouin zone in Fig. 2(a). The flat band of interest, E_{fp} , is the highest energy band and does not feature any band touchings when $t_{fp}^2 > 3t_p t_f$. We will assume that this is the case below. In Fig. 2(b), the energy of the top band with a μ_f shift is plotted as a function of $\mu_f - \mu_f^c$ and k_y , showing a flat band at $\mu_f = \mu_f^c$.

III. FERROMAGNETIC PERCOLATION IN INTERACTING FLAT BANDS

Before discussing the main result, we first briefly review the percolation representation in the Hubbard model studied by Mielke and Tasaki [1]. We then present and prove our results for the model in Sec. II, where the presence of Hund's coupling plays an important role.

A. Mielke-Tasaki Percolation in Flat Band Hubbard Models

For a system where the lowest-energy single-particle band is flat, a percolation representation of ferromagnetism in the flat band was found in Ref. [1] in terms of a linearly independent set of N_d states $\{\varphi_u(\mathbf{r})\}$ spanning the space of the flat band. In this notation, \mathbf{r} is a lattice site and u labels the state φ_u . The index set of all state labels u is denoted Λ_φ . The percolation representation applies under two further conditions. First is *quasilocality*, which requires each single-particle state to have a special site in its support where every other state vanishes, i.e., for each u there is an \mathbf{r}_u^* such that $\varphi_v(\mathbf{r}_u^*) \neq 0$ if and only if $v = u$. Second is that no more than two states can overlap at any site, i.e., for any site \mathbf{r} there are at most two states u and v such that $\varphi_u(\mathbf{r}) \neq 0$ and $\varphi_v(\mathbf{r}) \neq 0$. Two states u and v are said to be *directly connected* or *overlapping* if there is such a site \mathbf{r} where both states are nonzero.

Under these conditions, Ref. [1] found that if the number of electrons satisfies $N_e \leq N_d$, the ground states of the interacting system in the presence of a repulsive single-orbital Hubbard interaction can be written as a linear superposition of states formed from clusters of single-particle states with maximum total spin.

The ground state space being spanned by the cluster states yields a percolation representation where typical ground states are paramagnetic at low filling and ferromagnetic at high filling. If filling is low, a typical ground state consists of small, independent clusters that individually maximize spin but can have low total spin. If filling is high, there is typically one macroscopic cluster dominating the total spin. In particular, if $N_e = N_d$, the ground state space is spanned by fully spin-polarized states with trivial spin degeneracy. The above result from Ref. [1] thus allows for a filling-dependent ferromagnetic transition to be studied by treating the transition as a geometric percolation problem with additional spin weights due to the cluster S_z degeneracy [17].

This percolation representation was proven by constructing N_e -particle interacting states from single-particle flat band states and requiring the interacting states to have minimum Hubbard interaction energy, giving a ground state of the interacting system since the flat band minimizes the kinetic energy. In the proof of this result, the quasilocality condition is used to prevent double occupation of single-particle states, and the requirement that an overlap between single-particle states at a particular site involves only two states u and v yields the fact that the overall state is symmetric under swapping the spins of u and v , indicating maximum total spin in the cluster. Violating either of these conditions can lead to clusters with lower total spin that still have zero interaction energy.

For the model in Sec. II, the localized states shown in Fig. 1 satisfy quasilocality, as only one such state is nonzero at each f orbital, but the conditions of the above

theorem do not hold since three single-particle states have nonzero amplitude in the p_y orbital component on each honeycomb lattice site $\mathbf{r} \in \Lambda_p$. Thus, just the interaction H_U is insufficient to produce a percolation representation of maximum-spin clusters in our multi-orbital model, and we will find that the combination of H_U and H_J allows for a percolation representation. We note as well that the f orbitals allowing quasilocality to be satisfied in the basis of localized states $|\psi_{\mathbf{R},\sigma}\rangle$ is necessary to find a percolation representation in terms of these localized states. Using features of the proof of our main result in Sec. IIIB, we demonstrate in Appendix A an explicit example with a lower-than-maximum-spin cluster for the flat bands of the p -orbital Hamiltonian H_K^p even when intra-orbital Hubbard interactions and Hund's coupling are both considered.

B. Percolation representation with Hund's coupling

We will now see, by studying the model in Sec. II that a multi-orbital extension of the argument in Ref. [1] together with Hund's coupling can lead to a percolation representation that supports a ferromagnetic transition even when there is an overlap between more than two localized states. The argument then proceeds as follows. First, we perform a particle-hole transformation to study a model with a lowest-energy flat band. Next, we write an arbitrary ground state as a superposition of N_e -particle states in the localized state basis. Then, we require the ground state to be a zero-energy eigenstate of the intra-orbital Hubbard interaction in the p_x and p_y orbitals as well as of the Hund's coupling. This will show that when the particle-hole-transformed flat band is at most half filled, the ground state space is spanned by states with maximum-spin clusters. Finally, we invert the particle-hole transformation to show that when the highest-energy flat band of the original system is at least half filled, the ground state space is also spanned by states with maximum-spin clusters.

Let us first define a creation operator $a_{\mathbf{R},\sigma}^\dagger$ for a localized state centered at site $\mathbf{R} \in \Lambda_f$,

$$\begin{aligned} a_{\mathbf{R},\sigma}^\dagger &\equiv \sum_{\mathbf{R} \in \Lambda_f} \varphi_{\mathbf{R}}(\mathbf{R}, f) c_\sigma^\dagger(\mathbf{R}, f) + \sum_{\substack{\mathbf{r} \in \Lambda_p \\ p=p_x, p_y}} \varphi_{\mathbf{R}}(\mathbf{r}, p) c_\sigma^\dagger(\mathbf{r}, p) \\ &\equiv \boldsymbol{\varphi}_{\mathbf{R}} \cdot \mathbf{c}_\sigma^\dagger, \end{aligned} \tag{10}$$

with $\mathbf{c}_\sigma^\dagger$ a compact notation for f -, p_x -, and p_y -orbital electron creation operators on the entire lattice Λ as a $(|\Lambda_f| + 2|\Lambda_p|)$ -component vector. The wavefunction $\boldsymbol{\varphi}_{\mathbf{R}}$ is compactly supported, taking nonzero values only for the f orbital at \mathbf{R} and the p_x and p_y orbitals at $\mathbf{R} + \mathbf{u}_i$ with $i = 1, 2, \dots, 6$. Due to the localized state structure with p orbitals perpendicular to the outgoing bonds, the p_x components vanish at $\mathbf{R} + \mathbf{u}_1$ and $\mathbf{R} + \mathbf{u}_4$ as well. In this notation, a component of $\mathbf{c}_\sigma^\dagger$ will be labeled $c_\sigma^\dagger(\mathbf{r}, \sigma_r)$

where \mathbf{r} is a site on the lattice and $o_{\mathbf{r}}$ is the orbital index at that site. Thus, if $\mathbf{r} = \mathbf{R} \in \Lambda_f$, $o_{\mathbf{r}} = f$ and $c_{\sigma}^{\dagger}(\mathbf{R}, f) = f_{\mathbf{R},\sigma}^{\dagger}$. Similarly, there are two operators corresponding to $o_{\mathbf{r}} = p_x$ and $o_{\mathbf{r}} = p_y$ if $\mathbf{r} \in \Lambda_p$. The dot product notation is a shorthand for summing over all sites and orbitals. The subscript $\mathbf{R} \in \Lambda_f$ in $\varphi_{\mathbf{R}}$ identifies the localized state centered at \mathbf{R} .

The maximum-spin cluster states that will span the ground state space for appropriate filling are defined by selecting a subset $A \subset \Lambda_f$ and placing one single-particle localized state $\varphi_{\mathbf{R}}$ at each $\mathbf{R} \in A$. The set A can then be partitioned into $A = \bigsqcup_{k=1}^n C_k$, where C_k are disjoint clusters, and two states labeled by $\mathbf{R}, \mathbf{R}' \in A$ belong to the same cluster if they are overlapping or connected by a path of overlapping states. Since total spin is maximized within each cluster, these states can be constructed from states $|\Phi_{A\uparrow}\rangle = \prod_{\mathbf{R} \in A} a_{\mathbf{R},\uparrow}^{\dagger} |0\rangle$ or $|\Phi_{A\uparrow}^{(h)}\rangle = \prod_{\mathbf{R} \in A} a_{\mathbf{R},\uparrow} |F\rangle$ with $|F\rangle = \prod_{\mathbf{r} \in \Lambda} \prod_{o_{\mathbf{r}}} c_{\uparrow}^{\dagger}(\mathbf{r}, o_{\mathbf{r}}) c_{\downarrow}^{\dagger}(\mathbf{r}, o_{\mathbf{r}}) |0\rangle$ the fully filled state, depending on whether the flat band is the lowest- or highest-energy band.

For the particle-hole transformed Hamiltonian, where the flat band is the lowest-energy band, the S_z spin of each cluster can be lowered by a cluster spin-lowering operator $S_{C_k}^- = \sum_{(\mathbf{r}, o_{\mathbf{r}}) \in V_k} S_{\mathbf{r}, o_{\mathbf{r}}}^-$ with $S_{\mathbf{r}, o_{\mathbf{r}}}^- = c_{\downarrow}^{\dagger}(\mathbf{r}, o_{\mathbf{r}}) c_{\uparrow}(\mathbf{r}, o_{\mathbf{r}})$ acting on $V_k = \{(\mathbf{r}, o_{\mathbf{r}}) | \varphi_{\mathbf{R}}(\mathbf{r}, o_{\mathbf{r}}) \neq 0 \text{ for any } \mathbf{R} \in C_k\}$, the set of orbitals where at least one state in the cluster is nonzero. For the original Hamiltonian, where the flat band is the highest-energy band, the analogous operator acting on holes is $S_{C_k}^{(h)-} = \sum_{(\mathbf{r}, o_{\mathbf{r}}) \in V_k} c_{\downarrow}(\mathbf{r}, o_{\mathbf{r}}) c_{\uparrow}^{\dagger}(\mathbf{r}, o_{\mathbf{r}})$.

For the particle-hole transformed Hamiltonian, found by replacing creation and annihilation operators $f_{\mathbf{R},\sigma} \leftrightarrow f_{\mathbf{R},\sigma}^{\dagger}$, $p_{\mathbf{r},\hat{x},\sigma} \leftrightarrow p_{\mathbf{r},\hat{x},\sigma}^{\dagger}$, and $p_{\mathbf{r},\hat{y},\sigma} \leftrightarrow p_{\mathbf{r},\hat{y},\sigma}^{\dagger}$ in H , we find the following theorem.

Theorem 1 Consider the particle-hole transformed Hamiltonian $H^{(ph)} = -H_K + H_U + H_J - \frac{J}{2} \hat{N}_p - H_{\mu}$ with $t_{fp}^2 > 3t_p t_f$ and $t_p, t_f, t_{fp}, U_p, U_f, J > 0$. When $N_e \leq |\Lambda_f|$ and $\mu_f = \mu_f^{(ph),c} \equiv \mu_f^c + U_f/2 - U_p/2 + J/2$, with μ_f^c defined in Eq. (8), the ground state space of $H^{(ph)}$ is spanned by the states

$$|\Phi_{A,\{m_k\}}^{(ph)}\rangle = \prod_{k=1}^n (S_{C_k}^-)^{\lfloor \frac{|C_k|}{2} - m_k \rfloor} |\Phi_{A\uparrow}\rangle \quad (11)$$

with $A \subset \Lambda_f$ and $|A| = N_e$.

One important detail is that the required μ_f in Theorem 1 is not the μ_f^c for which H_K has a highest-energy flat band. Instead, there is a shift due to the additional chemical potential terms in the particle-hole-symmetric H_U and the particle-hole-transformed Hund's coupling $H_J - \frac{J}{2} \hat{N}_p$. When $\mu_f = \mu_f^{(ph),c}$, the single-particle terms in $H^{(ph)}$ have a lowest-energy flat band spanned by the set of states $\{\varphi_{\mathbf{R}}\}_{\mathbf{R} \in \Lambda_f}$. We have discarded additional

constant terms in $H^{(ph)}$, as they will not affect the spectrum or chemical potential condition.

For our original model, we find the following theorem.

Theorem 2 Consider H defined in Sec. II with $t_{fp}^2 > 3t_p t_f$ and $t_p, t_f, t_{fp}, U_p, U_f, J > 0$. When $N_e \geq 4|\Lambda_p| + |\Lambda_f|$ and $\mu_f = \mu_f^{(ph),c}$, defined in Theorem. 1, the ground state space of H is spanned by

$$|\Phi_{A,\{m_k\}}\rangle = \prod_{k=1}^n (S_{C_k}^{(h)-})^{\lfloor \frac{|C_k|}{2} - m_k \rfloor} |\Phi_{A\uparrow}^{(h)}\rangle, \quad (12)$$

where $A \subset \Lambda_f$, $|A| = N_e$, and $A = \bigsqcup_{k=1}^n C_k$ where C_k are disjoint clusters.

We now proceed with the proof of Theorem 1, from which, our main result, Theorem 2 immediately follows by a particle-hole transformation. Importantly, the basis states $|\Phi_{A,\{m_k\}}\rangle$ feature maximum total spin within each cluster, since $|\Phi_{A,\{m_k\}}\rangle$ is a particle-hole transformation of $|\Phi_{A,\{m_k\}}^{(ph)}\rangle$ and total spin commutes with particle-hole transformations, as reviewed in Appendix C.

Proof: Following Ref. [1], we construct operators canonically conjugate to $a_{\mathbf{R},\sigma}^{\dagger}$ by defining

$$b_{\mathbf{R},\sigma} = \kappa_{\mathbf{R}} \cdot \mathbf{c}_{\sigma},$$

$$\kappa_{\mathbf{R}}(\mathbf{r}, o_{\mathbf{r}}) = \sum_{\mathbf{R}' \in \Lambda_f} (G^{-1})_{\mathbf{R},\mathbf{R}'} \varphi_{\mathbf{R}'}(\mathbf{r}, o_{\mathbf{r}}), \quad (13)$$

with $G_{\mathbf{R},\mathbf{R}'} = \varphi_{\mathbf{R}} \cdot \varphi_{\mathbf{R}'}$ the Gram matrix for the states $\varphi_{\mathbf{R}}$. Thus, $\kappa_{\mathbf{R}} \cdot \varphi_{\mathbf{R}'} = \delta_{\mathbf{R},\mathbf{R}'}$ implies the canonical anticommutation relation $\{b_{\mathbf{R}',\sigma'}, a_{\mathbf{R},\sigma}^{\dagger}\} = \delta_{\mathbf{R},\mathbf{R}'} \delta_{\sigma,\sigma'}$. The states $\kappa_{\mathbf{R}}$ serve as an alternate basis for the flat band, and this Gram matrix procedure is essentially a method of constructing a dual basis where each element of the dual basis is orthogonal to all but one of the vectors in the original basis. This procedure is similar to the construction of reciprocal lattice vectors from direct lattice vectors.

Now $c_{\sigma}(\mathbf{r}, o_{\mathbf{r}})$ can be expressed in terms of $b_{\mathbf{R}}$ by multiplying by $\varphi_{\mathbf{R}}(\mathbf{r}, o_{\mathbf{r}})$ and summing over \mathbf{R} , an operator $d_{\sigma}(\mathbf{r}, o_{\mathbf{r}})$ can be defined to express the electron annihilation operators as

$$c_{\sigma}(\mathbf{r}', o'_{\mathbf{r}'}) = \sum_{\mathbf{R} \in \Lambda_f} \varphi_{\mathbf{R}}(\mathbf{r}, o_{\mathbf{r}}) b_{\mathbf{R},\sigma} - d_{\sigma}(\mathbf{r}, o_{\mathbf{r}}), \quad (14)$$

where $d_{\sigma}(\mathbf{r}, o) = \sum_{\mathbf{r}' \in \Lambda} \psi(\mathbf{r}, o_{\mathbf{r}}; \mathbf{r}', o'_{\mathbf{r}'}) c_{\sigma}(\mathbf{r}', o'_{\mathbf{r}'})$ with $\psi(\mathbf{r}, o_{\mathbf{r}}; \mathbf{r}', o'_{\mathbf{r}'}) \equiv \delta_{\mathbf{r},\mathbf{r}'} \delta_{o_{\mathbf{r}}, o'_{\mathbf{r}'}} - \sum_{\mathbf{R} \in \Lambda_f} \varphi_{\mathbf{R}}(\mathbf{r}, o_{\mathbf{r}}) \kappa_{\mathbf{R}}(\mathbf{r}', o'_{\mathbf{r}'})$ a projection onto of the flat band spanned by $\varphi_{\mathbf{R}}$ and $\kappa_{\mathbf{R}}$. Thus, $\{d_{\sigma}(\mathbf{r}, o_{\mathbf{r}}), a_{\mathbf{R},\sigma}^{\dagger}\} = \{d_{\sigma}(\mathbf{r}, o_{\mathbf{r}}), b_{\mathbf{R},\sigma}^{\dagger}\} = 0$. Since the ground state will be expressed in terms of $a_{\mathbf{R},\sigma}^{\dagger}$ operators, this construction allows the ground state condition in the presence of interactions to be analyzed using only states orthogonal or canonically conjugate to the single-particle localized flat band states.

When it is possible to construct an N_e -electron state from single-particle flat band states that simultaneously

minimizes the interactions, such a state will be a ground state, and the ground state space will be spanned by the collection of these states. In particular, the $n_\uparrow n_\downarrow$ interaction H'_J and H_J are positive semidefinite, so when there are states satisfying $H'_J|\Phi\rangle = H_J|\Phi\rangle = 0$ with energy $-N_e E_{fp}$, these states will be ground states of $H^{(ph)}$ and can be written

$$|\Phi^{(ph)}\rangle = \sum_{A_\uparrow, A_\downarrow \subset \Lambda_f} f(A_\uparrow, A_\downarrow) \prod_{\mathbf{R} \in A_\uparrow \sqcup A_\downarrow} \prod_{\sigma_{\mathbf{R}}} a_{\mathbf{R}, \sigma_{\mathbf{R}}}^\dagger |0\rangle, \quad (15)$$

with constraints on the coefficients $f(A_\uparrow, A_\downarrow)$ to be determined by the zero-interaction-energy conditions. Here A_\uparrow and A_\downarrow are subsets of Λ_f and $\sigma_{\mathbf{R}} = \uparrow$ or \downarrow if $\mathbf{R} \in A_\uparrow$ or $\mathbf{R} \in A_\downarrow$. If $\mathbf{R} \in A_\uparrow \cap A_\downarrow$, the product over $\sigma_{\mathbf{R}}$ includes both, with the spin-up operator to the left. The sum over A_\uparrow, A_\downarrow is a sum over all possible such subsets satisfying $|A_\uparrow| + |A_\downarrow| = N_e$. We will see that $|\Phi^{(ph)}\rangle = 0$ if $N_e > |\Lambda_f|$.

Since H'_J and H_J are themselves sums of positive-semidefinite operators at each site, we first consider the Hubbard interaction on an f orbital at \mathbf{R} , which gives the condition

$$\begin{aligned} 0 &= c_\uparrow(\mathbf{R}, f) c_\downarrow(\mathbf{R}, f) |\Phi^{(ph)}\rangle \\ &= \left(d_\uparrow(\mathbf{R}, f) + \sum_{\mathbf{R}' \in \Lambda_f} \varphi_{\mathbf{R}'}(\mathbf{R}, f) b_{\mathbf{R}', \uparrow} \right) \\ &\quad \times \left(d_\downarrow(\mathbf{R}, f) + \sum_{\mathbf{R}'' \in \Lambda_f} \varphi_{\mathbf{R}''}(\mathbf{R}, f) b_{\mathbf{R}'', \downarrow} \right) |\Phi^{(ph)}\rangle \\ &\implies b_{\mathbf{R}, \uparrow} b_{\mathbf{R}, \downarrow} |\Phi^{(ph)}\rangle = 0, \end{aligned} \quad (16)$$

since $d_\sigma(\mathbf{r}, \sigma_{\mathbf{r}})$ anticommutes with $b_{\mathbf{R}, \sigma}$ and with the $a_{\mathbf{R}, \sigma}^\dagger$ operators in $|\Phi\rangle$, and $\varphi_{\mathbf{R}'}(\mathbf{R}, f) \neq 0$ only when $\mathbf{R}' = \mathbf{R}$. Thus, since this condition holds for any $\mathbf{R} \in \Lambda_f$, the state $|\Phi^{(ph)}\rangle$ must satisfy $f(A_\uparrow, A_\downarrow) = 0$ if $A_\uparrow \cap A_\downarrow \neq \emptyset$, or, in other words, there must be no double occupancy of localized single-particle states. If $N_e > |\Lambda_f|$, this condition can only be met if $|\Phi^{(ph)}\rangle = 0$, meaning the ground state cannot be expressed solely in terms of N_e flat band states and must have energy higher than $-N_e E_{fp}$.

Next, we examine the Hubbard interaction in the p_x and p_y orbitals. Consider a honeycomb cell labeled by $\mathbf{R}_0 \in \Lambda_f$ and examine its rightmost vertex, $\mathbf{r}_0 = \mathbf{R}_0 + \mathbf{u}_1$. Two additional honeycomb cells, centered at $\mathbf{R}_1 = \mathbf{R}_0 + \mathbf{w}_1$ and $\mathbf{R}_6 = \mathbf{R}_0 + \mathbf{w}_6$, share vertex \mathbf{r}_0 . The corresponding localized single-particle states $\varphi_{\mathbf{R}_i}$ have nonzero component in the p_y orbital at \mathbf{r}_0 for all three of $\mathbf{R}_0, \mathbf{R}_1$, and \mathbf{R}_6 , but only \mathbf{R}_1 and \mathbf{R}_6 have a nonzero p_x component at \mathbf{r}_0 . Excluding the normalization factor $t_f / \sqrt{6(t_f^2 + t_{fp}^2)}$ on the p -orbital components, the nonzero p_x components are, $\varphi_{\mathbf{R}_1}(\mathbf{r}_0, p_x) = -\frac{\sqrt{3}}{2}$ and $\varphi_{\mathbf{R}_6}(\mathbf{r}_0, p_x) = \frac{\sqrt{3}}{2}$ while the nonzero p_y components are $\varphi_{\mathbf{R}_0}(\mathbf{r}_0, p_y) = 1$, $\varphi_{\mathbf{R}_1}(\mathbf{r}_0, p_y) = -\frac{1}{2}$, and $\varphi_{\mathbf{R}_6}(\mathbf{r}_0, p_y) = -\frac{1}{2}$. No other localized states $\varphi_{\mathbf{R}}$ are nonzero at \mathbf{r}_0 .

The zero-interaction-energy condition for the p_x -orbital Hubbard interaction at site \mathbf{r}_0 is

$$\begin{aligned} 0 &= c_\uparrow(\mathbf{r}_0, p_x) c_\downarrow(\mathbf{r}_0, p_x) |\Phi^{(ph)}\rangle \\ &= \left(\sum_{i=1,6} \varphi_{\mathbf{R}_i}(\mathbf{r}_0, p_x) b_{\mathbf{R}_i, \uparrow} \right) \\ &\quad \times \left(\sum_{i=1,6} \varphi_{\mathbf{R}_i}(\mathbf{r}_0, p_x) b_{\mathbf{R}_i, \downarrow} \right) |\Phi^{(ph)}\rangle \\ &\implies (b_{\mathbf{R}_6, \uparrow} b_{\mathbf{R}_1, \downarrow} - b_{\mathbf{R}_6, \downarrow} b_{\mathbf{R}_1, \uparrow}) |\Phi^{(ph)}\rangle = 0, \end{aligned} \quad (17)$$

where the last line follows from the no-double-occupancy condition Eq. (16) and the fact that $\varphi_{\mathbf{R}_0}(\mathbf{r}_0, p_x) = 0$. The condition in Eq. (17) essentially projects out states involving a spin-singlet component between the states centered at \mathbf{R}_1 and \mathbf{R}_6 . Explicitly, this condition gives that for any configuration where $A_\uparrow = B_\uparrow \sqcup \{\mathbf{R}_1\}$ and $A_\downarrow = B_\downarrow \sqcup \{\mathbf{R}_6\}$ with $\mathbf{R}_1, \mathbf{R}_6 \notin B_\uparrow, B_\downarrow$, the coefficients are symmetric under exchange of spins, $f(B_\uparrow \sqcup \{\mathbf{R}_1\}, B_\downarrow \sqcup \{\mathbf{R}_6\}) = f(B_\uparrow \sqcup \{\mathbf{R}_6\}, B_\downarrow \sqcup \{\mathbf{R}_1\})$. Since the choice of \mathbf{R}_0 is arbitrary, this gives the general condition that the state must have spin exchange symmetry between localized single-particle states that are nearest neighbors in the y direction, states \mathbf{R} and $\mathbf{R}' = \mathbf{R} + \mathbf{w}_2$.

Eq. (16) and Eq. (17) are equivalent to the conditions resulting from quasilocality and the requirement that no more than two single-particle states overlap at any site in Ref. [1]. However, three states overlap in the p_y orbitals in the model we consider. For the p_y orbital at site \mathbf{r}_0 ,

$$\begin{aligned} 0 &= c_\uparrow(\mathbf{r}_0, p_y) c_\downarrow(\mathbf{r}_0, p_y) |\Phi^{(ph)}\rangle \\ &= \varphi_{\mathbf{R}_6}(\mathbf{r}_0, p_y) \varphi_{\mathbf{R}_0}(\mathbf{r}_0, p_y) (b_{\mathbf{R}_6, \uparrow} b_{\mathbf{R}_0, \downarrow} - b_{\mathbf{R}_6, \downarrow} b_{\mathbf{R}_0, \uparrow}) |\Phi^{(ph)}\rangle \\ &\quad + \varphi_{\mathbf{R}_1}(\mathbf{r}_0, p_y) \varphi_{\mathbf{R}_0}(\mathbf{r}_0, p_y) (b_{\mathbf{R}_1, \uparrow} b_{\mathbf{R}_0, \downarrow} - b_{\mathbf{R}_1, \downarrow} b_{\mathbf{R}_0, \uparrow}) |\Phi^{(ph)}\rangle \\ &\implies (b_{\mathbf{R}_6, \uparrow} b_{\mathbf{R}_0, \downarrow} - b_{\mathbf{R}_6, \downarrow} b_{\mathbf{R}_0, \uparrow}) |\Phi^{(ph)}\rangle \\ &\quad + (b_{\mathbf{R}_1, \uparrow} b_{\mathbf{R}_0, \downarrow} - b_{\mathbf{R}_1, \downarrow} b_{\mathbf{R}_0, \uparrow}) |\Phi^{(ph)}\rangle = 0, \end{aligned} \quad (18)$$

using Eq. (16) and Eq. (17). While this condition is satisfied for states that maximize spin (have spin exchange symmetry) between single-particle states at \mathbf{R}_6 and \mathbf{R}_0 as well as between those at \mathbf{R}_1 and \mathbf{R}_0 , it is not the case that every state $|\Phi\rangle$ satisfying Eq. (18) must have such spin exchange symmetry. Thus, the percolation representation is not strictly valid when the only interaction is H'_J .

The final condition we consider is $H_J|\Phi\rangle = 0$. This condition can be written using only annihilation operators in H_J by writing $H_J = \frac{J}{2} \sum_{\mathbf{r} \in \Lambda_p} n_{\mathbf{r}, S=0}$, where $n_{\mathbf{r}, S=0} = (p_{\mathbf{r}, \hat{y}, \downarrow}^\dagger p_{\mathbf{r}, \hat{x}, \uparrow}^\dagger - p_{\mathbf{r}, \hat{y}, \uparrow}^\dagger p_{\mathbf{r}, \hat{x}, \downarrow}^\dagger) (p_{\mathbf{r}, \hat{x}, \uparrow} p_{\mathbf{r}, \hat{y}, \downarrow} - p_{\mathbf{r}, \hat{x}, \downarrow} p_{\mathbf{r}, \hat{y}, \uparrow}) \equiv c_{\mathbf{r}, S=0}^\dagger c_{\mathbf{r}, S=0}$ is an operator that counts whether there is a spin singlet between the p_x and p_y orbitals at site \mathbf{r} . The derivation of this operator identity is shown in Appendix B. In this form, H_J is clearly a sum of positive semidefinite operators, and $H_J|\Phi\rangle = 0$ if and only if $c_{\mathbf{r}, S=0}|\Phi\rangle = 0$ for every $\mathbf{r} \in \Lambda_p$.

In terms of localized state operators, the zero-interaction-energy condition for Hund's coupling at site \mathbf{r}_0 is

$$\begin{aligned}
0 &= [c_\uparrow(\mathbf{r}_0, p_x)c_\downarrow(\mathbf{r}_0, p_y) - c_\downarrow(\mathbf{r}_0, p_x)c_\uparrow(\mathbf{r}_0, p_y)]|\Phi^{(ph)}\rangle \\
&= \varphi_{\mathbf{R}_6}(\mathbf{r}_0, p_x)\varphi_{\mathbf{R}_0}(\mathbf{r}_0, p_y)(b_{\mathbf{R}_6, \uparrow}b_{\mathbf{R}_0, \downarrow} - b_{\mathbf{R}_6, \downarrow}b_{\mathbf{R}_0, \uparrow})|\Phi^{(ph)}\rangle \\
&+ \varphi_{\mathbf{R}_1}(\mathbf{r}_0, p_x)\varphi_{\mathbf{R}_0}(\mathbf{r}_0, p_y)(b_{\mathbf{R}_1, \uparrow}b_{\mathbf{R}_0, \downarrow} - b_{\mathbf{R}_1, \downarrow}b_{\mathbf{R}_0, \uparrow})|\Phi^{(ph)}\rangle \\
&\implies (b_{\mathbf{R}_6, \uparrow}b_{\mathbf{R}_0, \downarrow} - b_{\mathbf{R}_6, \downarrow}b_{\mathbf{R}_0, \uparrow})|\Phi^{(ph)}\rangle \\
&\quad - (b_{\mathbf{R}_1, \uparrow}b_{\mathbf{R}_0, \downarrow} - b_{\mathbf{R}_1, \downarrow}b_{\mathbf{R}_0, \uparrow})|\Phi^{(ph)}\rangle,
\end{aligned} \tag{19}$$

using the no-double-occupancy condition from Eq. (16) and the spin triplet condition between \mathbf{R}_1 and \mathbf{R}_6 from Eq. (17). Taking the sum and difference of the conditions in Eqs. (18) and (19) gives spin triplet conditions between \mathbf{R}_0 and \mathbf{R}_1 and between \mathbf{R}_0 and \mathbf{R}_6 . In other words, the spin degree of freedom must be fully symmetrized among any overlapping states at \mathbf{r}_0 . This argument holds for any choice of \mathbf{R}_0 , meaning it applies at any site in the same honeycomb sublattice as \mathbf{r}_0 . In fact, as can be seen by considering the left-most site on the \mathbf{R}_0 -centered honeycomb, $\mathbf{r}'_0 = \mathbf{R}_0 + \mathbf{u}_4$, these spin symmetrization conditions apply both sublattices of the p -orbital honeycomb lattice Λ_p . If spin must be symmetrized between any two overlapping localized states, a cluster of localized states will be fully spin symmetrized, since any two localized states in a cluster can be connected by a path of overlapping localized states each adjacent pair of which must have symmetrized spin. Thus, clusters of localized states have maximum total spin $S_{C_k, tot} = \frac{|C_k|}{2}$ and ground states for $N_e \leq |\Lambda_f|$ can be written in the form of Eq. (11). ■

Theorem 2 follows immediately by particle-hole transformation. In particular, since Theorem 1 requires the lowest-energy flat band to be *at most* half filled, Theorem 2 requires the highest-energy flat band to be *at least* half filled. The clusters in Eq. (12) are then connected sets of singly-occupied localized states surrounded by a doubly-occupied background.

In order to interpret Theorem 2 as a percolation representation, note that when the highest-energy flat band is exactly half filled, $|N_e| = 4|\Lambda_p| + |\Lambda_f|$, there is a single cluster spanning the system, and all ground states have total spin $\frac{|\Lambda_f|}{2}$. When the system is close to fully filled, clusters are small and it is easy to find combinations of basis states in Eq. (12) with low total spin. As the highest-energy flat band approaches half filling, the ground state space becomes dominated by states with a large cluster spanning the system and carrying large spin. There is thus a paramagnetic-ferromagnetic transition as the system approaches half filling of the top band from above in the sense that sufficiently close to half filling, the ground state space is dominated by states with macroscopic spin.

The percolation transition can be found through Monte Carlo simulation [17]. Since the localized single-particle states can be labeled by their f orbital sites, the perco-

lation picture involves filled or empty sites on the triangular lattice Λ_f , with adjacent filled sites on the triangular lattice belonging to the same cluster. This can be thought of as a percolation of hole states with N_h holes in the otherwise fully-filled system. In this percolation picture, physical quantities are computed by averaging over the degenerate ground state space. In particular, the expected value of the spin in each basis state is

$$S_A^2 \equiv \langle \Phi_{A, \{m_k\}}^h | S^2 | \Phi_{A, \{m_k\}}^h \rangle = \sum_{k=1}^n \frac{|C_k|}{2} \left(\frac{|C_k|}{2} + 1 \right), \tag{20}$$

which depends only on the sizes of the n clusters. The percolation transition is signalled by the filling at which $\langle S^2 \rangle / S_{max}^2$ becomes nonzero in the thermodynamic limit, where the maximum value $S_{max}^2 = \frac{N_h}{2} \left(\frac{N_h}{2} + 1 \right)$ occurs for configurations with only a single cluster.

IV. CONCLUSIONS

We have studied a multi-orbital model with two layers, one a honeycomb lattice layer with p_x and p_y orbitals and the other a triangular lattice layer of $f_{y(3x^2-y^2)}$ orbitals with triangular lattice vertices aligned with the centers of the p -orbital honeycomb plaquettes. For an appropriate chemical potential difference between the two layers, the system admits a flat band spanned by single-particle states localized to each f orbital and the surrounding p -orbital plaquette. We proved that when this flat band is the highest-energy band, the ground state space of the system with intra-orbital Hubbard interactions and Hund's coupling is spanned by states with maximum-spin clusters when the flat band is at least half filled. The completeness of this cluster state basis allows for a percolation representation, where the system is paramagnetic far from and ferromagnetic near half filling of the flat band. In particular, when the flat band is exactly half filled, the ground states are fully spin polarized.

ACKNOWLEDGMENTS

We thank Tyrel McQueen for helpful discussion. This work is supported by the NSF CAREER grant DMR-1848349 and in part by the Alfred P. Sloan Research Fellowships under grant FG-2018-10971.

Appendix A: Lower-spin Clusters in p -orbital System

In this appendix, we consider just the p -orbital Hamiltonian $H = H_K^p + H_U + H_J$, with the intra-orbital Hubbard interactions in the p_x and p_y orbitals as well as Hund's coupling. By use of a simple example, we show that the loop state basis $|\psi_{\mathbf{R}, \sigma}^{-(p)}\rangle$ does not admit a simple percolation picture, as there are states where clusters do

not maximize total spin. For consistency, we use the notation from Sec. III B with the modification that there are no f orbital sites and Λ_f is simply the set of honeycomb plaquette labels. Thus, $\varphi_{\mathbf{R}}(\mathbf{r}, o_{\mathbf{r}})$ describes the component at orbital $o_{\mathbf{r}} = p_x, p_y$ of site \mathbf{r} of a loop state on the plaquette \mathbf{R} . All operators $a_{\mathbf{R},\sigma}$ and $b_{\mathbf{R},\sigma}$ are defined similarly to in Sec. III B using the wavefunctions $\varphi_{\mathbf{R}}(\mathbf{r}, o_{\mathbf{r}})$ defined only at sites $\mathbf{r} \in \Lambda_p$.

Consider an arbitrary plaquette centered at \mathbf{R}_0 together with the six surrounding plaquettes centered at $\mathbf{R}_i = \mathbf{R}_0 + \mathbf{w}_i$ with $i = 1, \dots, 6$. The nonzero components at site $\mathbf{r}_1 = \mathbf{R}_0 + \mathbf{u}_1$ are $\varphi_{\mathbf{R}_1}(\mathbf{r}_1, p_x) = -\frac{\sqrt{3}}{2}$ and $\varphi_{\mathbf{R}_6}(\mathbf{r}_1, p_x) = \frac{\sqrt{3}}{2}$ while the nonzero p_y components are $\varphi_{\mathbf{R}_0}(\mathbf{r}_1, p_y) = 1$, $\varphi_{\mathbf{R}_1}(\mathbf{r}_1, p_y) = -\frac{1}{2}$, and $\varphi_{\mathbf{R}_6}(\mathbf{r}_1, p_y) = -\frac{1}{2}$, discarding the $1/\sqrt{6}$ normalization factor.

The equivalents of the interaction conditions in Eq. (17), (18), and (19) in this case are

$$\begin{aligned}
0 &= \left[b_{\mathbf{R}_1\uparrow} b_{\mathbf{R}_1\downarrow} + b_{\mathbf{R}_6\uparrow} b_{\mathbf{R}_6\downarrow} \right. \\
&\quad \left. - (b_{\mathbf{R}_1\uparrow} b_{\mathbf{R}_6\downarrow} - b_{\mathbf{R}_1\downarrow} b_{\mathbf{R}_6\uparrow}) \right] |\Phi\rangle \\
0 &= \left[4b_{\mathbf{R}_0\uparrow} b_{\mathbf{R}_0\downarrow} + b_{\mathbf{R}_1\uparrow} b_{\mathbf{R}_1\downarrow} + b_{\mathbf{R}_6\uparrow} b_{\mathbf{R}_6\downarrow} \right. \\
&\quad \left. + (b_{\mathbf{R}_1\uparrow} b_{\mathbf{R}_6\downarrow} - b_{\mathbf{R}_1\downarrow} b_{\mathbf{R}_6\uparrow}) - 2(b_{\mathbf{R}_0\uparrow} b_{\mathbf{R}_6\downarrow} - b_{\mathbf{R}_0\downarrow} b_{\mathbf{R}_6\uparrow}) \right. \\
&\quad \left. - 2(b_{\mathbf{R}_0\uparrow} b_{\mathbf{R}_1\downarrow} - b_{\mathbf{R}_0\downarrow} b_{\mathbf{R}_1\uparrow}) \right] |\Phi\rangle \\
0 &= \left[b_{\mathbf{R}_1\uparrow} b_{\mathbf{R}_1\downarrow} - b_{\mathbf{R}_6\uparrow} b_{\mathbf{R}_6\downarrow} + (b_{\mathbf{R}_0\uparrow} b_{\mathbf{R}_6\downarrow} - b_{\mathbf{R}_0\downarrow} b_{\mathbf{R}_6\uparrow}) \right. \\
&\quad \left. - (b_{\mathbf{R}_0\uparrow} b_{\mathbf{R}_1\downarrow} - b_{\mathbf{R}_0\downarrow} b_{\mathbf{R}_1\uparrow}) \right] |\Phi\rangle.
\end{aligned} \tag{A1}$$

These conditions reduce to the conditions in the main text when there are no doubly occupied states, meaning states where clusters of loop states maximize spin remain ground states. There are, however, linearly independent ground states that do not maximize spin due to having a doubly-occupied loop state. One such example is

$$|\Phi'_{\mathbf{R}_0}\rangle = a_{\mathbf{R}_0\uparrow}^\dagger \sum_{i=0}^6 a_{\mathbf{R}_i\downarrow}^\dagger |0\rangle. \tag{A2}$$

It can be verified that the state $|\Phi'_{\mathbf{R}_0}\rangle$ satisfies the three zero-interaction-energy conditions on every site. The conditions in Eq. (A1) are satisfied by $|\Phi'_{\mathbf{R}_0}\rangle$, and the conditions for the remaining sites can be shown to hold as well and follow from simple mappings. For example, the conditions at site $\mathbf{r}_2 = \mathbf{R}_0 + \mathbf{u}_2$ follow from replacing $\mathbf{R}_0 \rightarrow \mathbf{R}_1$, $\mathbf{R}_1 \rightarrow \mathbf{R}_0$, and $\mathbf{R}_6 \rightarrow \mathbf{R}_2$ in Eq. (A1).

The two-electron state $|\Phi'_{\mathbf{R}_0}\rangle$ includes a component where the state $\varphi_{\mathbf{R}_0}$ is doubly occupied and has total spin $\langle \Phi'_{\mathbf{R}_0} | S_{tot}^2 | \Phi'_{\mathbf{R}_0} \rangle / \langle \Phi'_{\mathbf{R}_0} | \Phi'_{\mathbf{R}_0} \rangle = \frac{6}{7}$. The percolation representation with maximum-spin clusters thus does not hold in the loop basis for H_K^p .

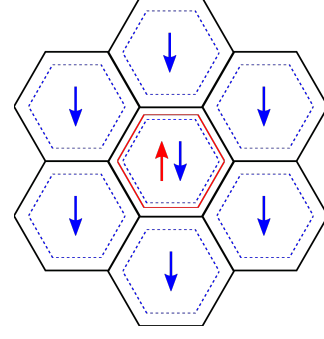


FIG. 3. Two-electron state $|\Phi'_{\mathbf{R}_0}\rangle$, which consists of a central filled spin-up loop surrounded by a superposition of spin-down loops on the central and six surrounding plaquettes. This state does not maximize spin despite avoiding the interaction energy.

Appendix B: Hund's Coupling Singlet Operator

The Hund's coupling term H_J is a sum of positive semidefinite operators at each honeycomb site,

$$\begin{aligned}
H_J &= \sum_{\mathbf{r} \in \Lambda_p} h_J(\mathbf{r}), \\
h_J(\mathbf{r}) &\equiv -J \left(\mathbf{S}_{\mathbf{r},p_x} \cdot \mathbf{S}_{\mathbf{r},p_y} - \frac{1}{4} n_{\mathbf{r},p_x} n_{\mathbf{r},p_y} \right)
\end{aligned} \tag{B1}$$

where $S_{\mathbf{r},p_x/y}^i = \frac{1}{2} \sum_{\mu,\nu=\uparrow,\downarrow} p_{\mathbf{r},\hat{x}/\hat{y},\mu}^\dagger \sigma_{\mu\nu}^i p_{\mathbf{r},\hat{x}/\hat{y},\nu}$ and $n_{\mathbf{r},p_x/y} = \sum_{\mu=\uparrow,\downarrow} p_{\mathbf{r},\hat{x}/\hat{y},\mu}^\dagger p_{\mathbf{r},\hat{x}/\hat{y},\mu}$. $h_J(\mathbf{r})$ takes its minimum eigenvalue of 0 when the p_x and p_y orbitals at site \mathbf{r} are singly occupied and form a spin triplet state, which can be seen explicitly by using the Pauli matrix completeness identity $\sum_{i=1}^3 \sigma_{\alpha\beta}^i \sigma_{\mu\nu}^i = 2\delta_{\alpha\nu} \delta_{\beta\mu} - \delta_{\alpha\beta} \delta_{\mu\nu}$ to write

$$\begin{aligned}
h_J(\mathbf{r}) &= -\frac{J}{4} \left[-n_{\mathbf{r},p_x} n_{\mathbf{r},p_y} + \sum_{\mu,\nu;\alpha,\beta=\uparrow,\downarrow} p_{\mathbf{r},\hat{x},\mu}^\dagger p_{\mathbf{r},\hat{x},\nu} p_{\mathbf{r},\hat{y},\alpha}^\dagger p_{\mathbf{r},\hat{y},\beta} (2\delta_{\alpha\nu} \delta_{\beta\mu} - \delta_{\alpha\beta} \delta_{\mu\nu}) \right] \\
&= \frac{J}{2} \left(n_{\mathbf{r},p_x,\uparrow} n_{\mathbf{r},p_y,\downarrow} + n_{\mathbf{r},p_x,\downarrow} n_{\mathbf{r},p_y,\uparrow} \right. \\
&\quad \left. - p_{\mathbf{r},\hat{x},\uparrow}^\dagger p_{\mathbf{r},\hat{x},\downarrow} p_{\mathbf{r},\hat{y},\downarrow}^\dagger p_{\mathbf{r},\hat{y},\uparrow} - p_{\mathbf{r},\hat{x},\downarrow}^\dagger p_{\mathbf{r},\hat{x},\uparrow} p_{\mathbf{r},\hat{y},\uparrow}^\dagger p_{\mathbf{r},\hat{y},\downarrow} \right) \\
&= -\frac{J}{2} \left(p_{\mathbf{r},\hat{x},\uparrow}^\dagger p_{\mathbf{r},\hat{y},\downarrow}^\dagger p_{\mathbf{r},\hat{x},\downarrow} p_{\mathbf{r},\hat{y},\uparrow} + p_{\mathbf{r},\hat{x},\downarrow}^\dagger p_{\mathbf{r},\hat{y},\uparrow}^\dagger p_{\mathbf{r},\hat{x},\uparrow} p_{\mathbf{r},\hat{y},\downarrow} \right) \\
&\quad \left. - p_{\mathbf{r},\hat{x},\uparrow}^\dagger p_{\mathbf{r},\hat{y},\downarrow}^\dagger p_{\mathbf{r},\hat{x},\downarrow} p_{\mathbf{r},\hat{y},\uparrow} - p_{\mathbf{r},\hat{x},\downarrow}^\dagger p_{\mathbf{r},\hat{y},\uparrow}^\dagger p_{\mathbf{r},\hat{x},\uparrow} p_{\mathbf{r},\hat{y},\downarrow} \right) \\
&= \frac{J}{2} (p_{\mathbf{r},\hat{y},\downarrow}^\dagger p_{\mathbf{r},\hat{x},\uparrow}^\dagger - p_{\mathbf{r},\hat{y},\uparrow}^\dagger p_{\mathbf{r},\hat{x},\downarrow}^\dagger) (p_{\mathbf{r},\hat{x},\uparrow} p_{\mathbf{r},\hat{y},\downarrow} - p_{\mathbf{r},\hat{x},\downarrow} p_{\mathbf{r},\hat{y},\uparrow}) \\
&\equiv \frac{J}{2} n_{\mathbf{r},S=0}.
\end{aligned} \tag{B2}$$

The Hund's coupling term can thus be written in terms of a sum of singlet number operators.

Appendix C: Particle-Hole Transformation and Total Spin

We show here for completeness that the particle-hole transformation and total spin operators commute. For notational simplicity, consider electron operators $c_{i\sigma}$, essentially absorbing both the site and orbital indices into the single index i . The total spin operator can be written

$$\begin{aligned}
 S_{tot}^2 &= \left(\sum_i \mathbf{S}_i \right)^2 \\
 &= \sum_{i,j} \sum_{\mu\nu\alpha\beta=\uparrow,\downarrow} c_{i\mu}^\dagger c_{i\nu} c_{j\alpha}^\dagger c_{j\beta} \boldsymbol{\sigma}_{\mu\nu} \cdot \boldsymbol{\sigma}_{\alpha\beta} \\
 &= \sum_{i,j} \sum_{\mu\nu\alpha\beta=\uparrow,\downarrow} (-c_{i\nu} c_{i\mu}^\dagger + \delta_{\mu\nu}) (-c_{j\beta} c_{j\alpha}^\dagger + \delta_{\alpha\beta}) \boldsymbol{\sigma}_{\mu\nu} \cdot \boldsymbol{\sigma}_{\alpha\beta} \\
 &= \sum_{i,j} \sum_{\mu\nu\alpha\beta=\uparrow,\downarrow} c_{i\nu} c_{i\mu}^\dagger c_{j\beta} c_{j\alpha}^\dagger \boldsymbol{\sigma}_{\mu\nu} \cdot \boldsymbol{\sigma}_{\alpha\beta} \\
 &= U^{(ph)\dagger} S_{tot}^2 U^{(ph)},
 \end{aligned} \tag{C1}$$

which follows from the tracelessness of σ^i and the fact that $\boldsymbol{\sigma}_{\mu\nu} \cdot \boldsymbol{\sigma}_{\alpha\beta} = \boldsymbol{\sigma}_{\nu\mu} \cdot \boldsymbol{\sigma}_{\beta\alpha}$. Thus, total spin is preserved by the particle-hole transformation.

-
- [1] A. Mielke and H. Tasaki, *Commun. Math. Phys.* **158**, 341 (1993).
- [2] A. Mielke, *J. Phys. A: Math. Gen.* **24**, L73 (1991).
- [3] C. Wu, D. Bergman, L. Balents, and S. Das Sarma, *Phys. Rev. Lett.* **99**, 070401 (2007).
- [4] E. Tang, J.-W. Mei, and X.-G. Wen, *Phys. Rev. Lett.* **106**, 236802 (2011).
- [5] R. Bistritzer and A. H. MacDonald, *PNAS* **108**, 12233 (2011).
- [6] Z. F. Wang, N. Su, and F. Liu, *Nano Letters* **13**, 2842 (2013), pMID: 23678979.
- [7] H. C. Po, L. Zou, A. Vishwanath, and T. Senthil, *Phys. Rev. X* **8**, 031089 (2018).
- [8] G. Tarnopolsky, A. J. Kruchkov, and A. Vishwanath, *Phys. Rev. Lett.* **122**, 106405 (2019).
- [9] D. L. Bergman, C. Wu, and L. Balents, *Phys. Rev. B* **78**, 125104 (2008).
- [10] M. Creutz, *Rev. Mod. Phys.* **73**, 119 (2001).
- [11] J. Zurita, C. E. Creffield, and G. Platero, *Advanced Quantum Technologies* **3**, 1900105 (2020).
- [12] C. S. Chiu, D.-S. Ma, Z.-D. Song, B. A. Bernevig, and A. A. Houck, (2020), arXiv:2010.11953 [cond-mat.mes-hall].
- [13] H. Tasaki, *Phys. Rev. Lett.* **69**, 1608 (1992).
- [14] A. Tanaka, *Journal of Statistical Physics* **181**, 897 (2020).
- [15] A. Mielke, *J. Phys. A: Math. Gen.* **24**, 3311 (1991).
- [16] A. Mielke, *J. Phys. A: Math. Gen.* **25**, 4335 (1992).
- [17] M. Maksymenko, A. Honecker, R. Moessner, J. Richter, and O. Derzhko, *Phys. Rev. Lett.* **109**, 096404 (2012).
- [18] R. Liu, W. Nie, and W. Zhang, *Science Bulletin* **64**, 1490 (2019).
- [19] C. Wu and S. Das Sarma, *Phys. Rev. B* **77**, 235107 (2008).
- [20] S. Zhang, H.-h. Hung, and C. Wu, *Phys. Rev. A* **82**, 053618 (2010).